Spintronic and optoelectronic devices using topological insulators and Dirac/Weyl materials

Hyunsoo Yang

Electrical and Computer Engineering, National University of Singapore

eleyang@nus.edu.sg

Outline

- Nanoelectronics overview
- Graphene magnetic sensors
- Graphene optoelectronics (THz devices)
- Spin-orbit torque (SOT) engineering
  - AHE & SOT in $LaAlO_3/SrTiO_3$ oxide heterostructures
  - SOT in topological insulators (Bi_2Se_3/ferromagnet)
- Topological insulator spin detectors
- Weyl spin lifetime measurements

2

Electron, photon, and spin

- Electronics
  - Transistor – small wavelength
  - FLASH memory – long trapping time

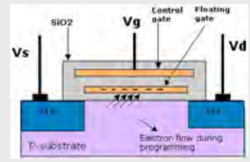

- Photonics
  - Optical fiber communication – long distance
  - Not compatible with nanoelectronic due to wavelength difference (diffraction limit)

- Spintronics
  - Information can be stored in magnetic materials.
  - Not easy to send for a long distance.

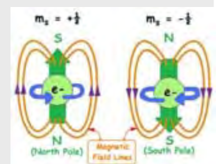

3

Grand challenges in electronics

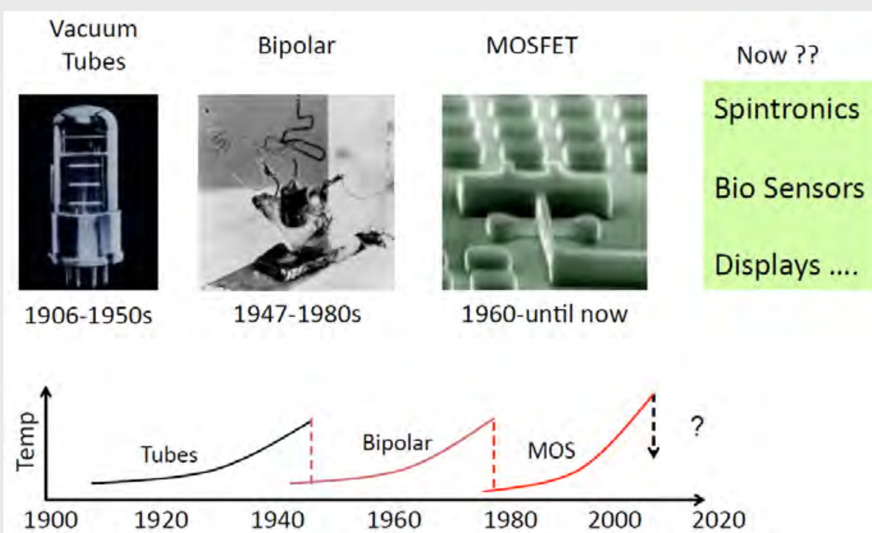

4

Emergence of electronics

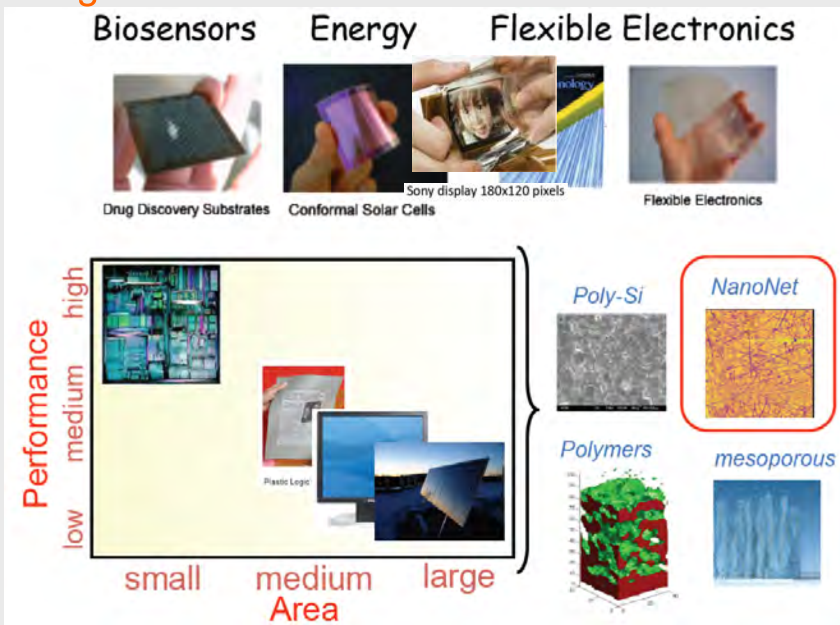

A difficult problem

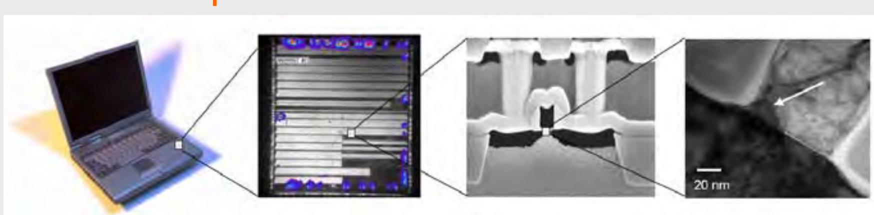

The ICs operate in incredibly harsh conditions, turning on and off trillions of time during its lifetime

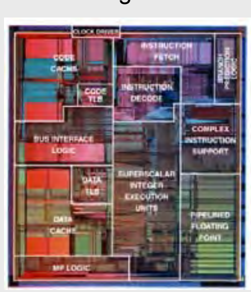

1 CPU ~ 10^9 Transistors

When one transistor fails, so does the IC

Uniformity issue is the challenge any new materials including graphene and 2D materials will face!

NUS National University of Singapore

Transistor scaling (lateral)

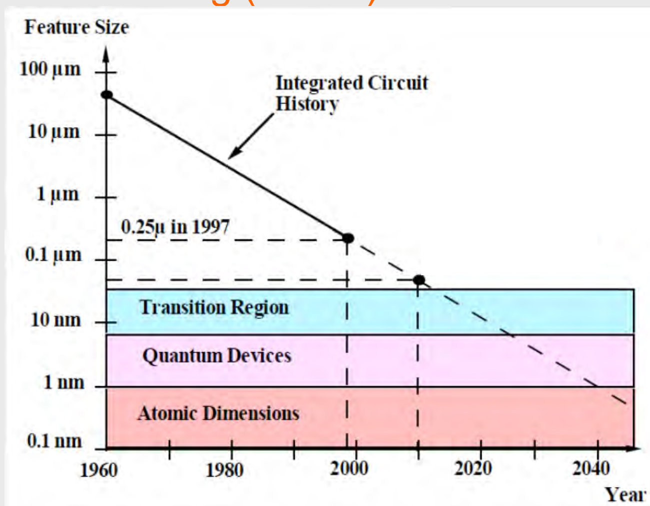

Devices are getting very small. Will they reach quantum or even atomic dimensions? What principles will they operate on? Still charge or is spin or something else possible?

NUS National University of Singapore

7

Thinner and thinner (vertical scaling)

graphite

graphene

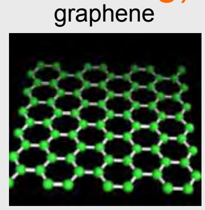

MoS_2
solid lubricant

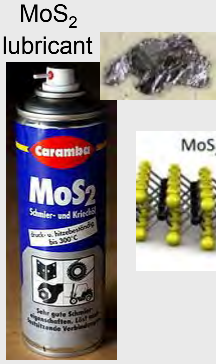

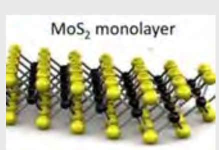

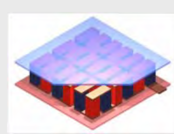

Bi_2Te_3 and Bi_2Se_3
Wine cooler

beveragefactory.com

Topological insulators

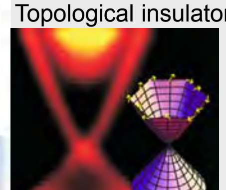

Physics 3, 62 (2010)

8

Graphene applications

A roadmap for graphene

K. S. Novoselov, V. I. Fal'ko, L. Colombo, P. R. Gellert, M. G. Schwab & K. Kim

192 | NATURE | VOL 490 | 11 OCTOBER 2012

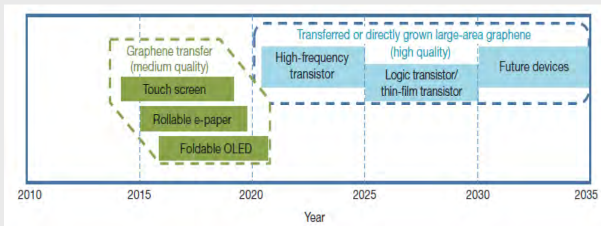

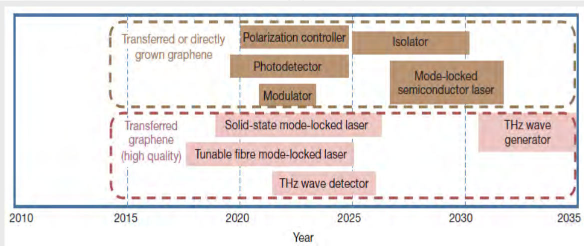

Sensors, optoelectronics (THz)

9

Why Silicon?

- **SiO_2 is a Magical Material**
  - SiO_2 passivates the surface of Si
  - SiO_2 is an excellent insulator
  - SiO_2 is an excellent barrier against impurity diffusion
  - SiO_2 has very high etch selectivity to Si
- Si is easily purified and can be grown defect free single crystal
- Si has reasonably good electronic properties which produce a variety of devices with excellent performance
- Si and SiO_2 are tolerant to a variety of harsh environments used in fabrication and is highly manufacturable
- Si has excellent mechanical properties which facilitate handling and manufacturing
- Si is readily available and very plentiful in nature

NUS National University of Singapore

10

Voltage controlled vs. current controlled

metal oxide semiconductor (MOS)

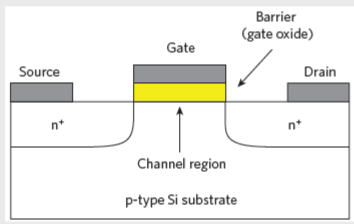

Voltage controlled (capacitive coupling)
Suitable for parallel connection

Spin transfer torque (STT)

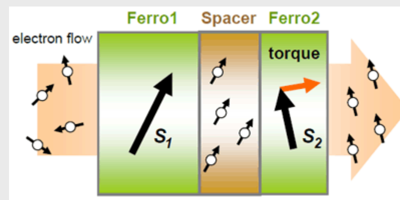

current controlled
Suitable for serial connection

Spin devices may not require an oxide layer
Need different approach

NUS National University of Singapore

Metal ions and alkali ions must be removed from Si device active regions

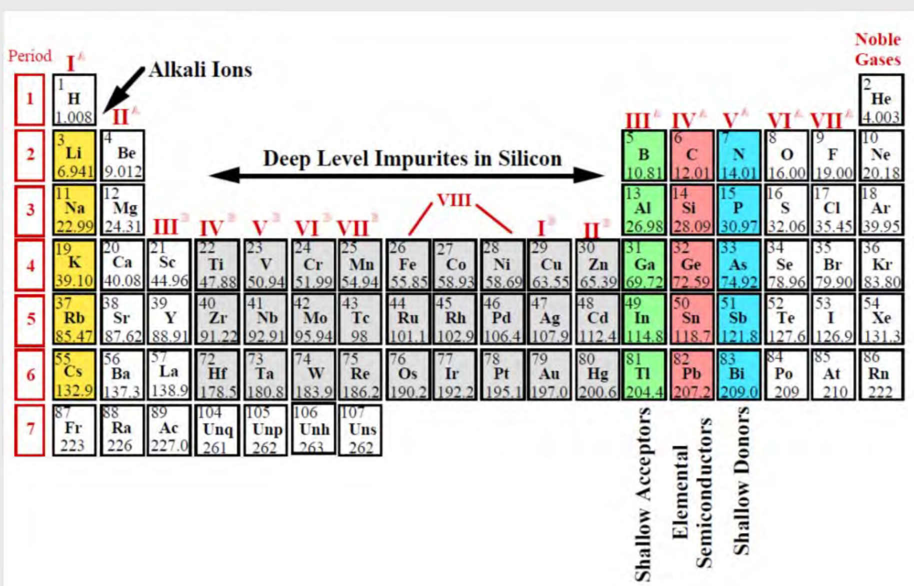

Technologically accessible photonic materials

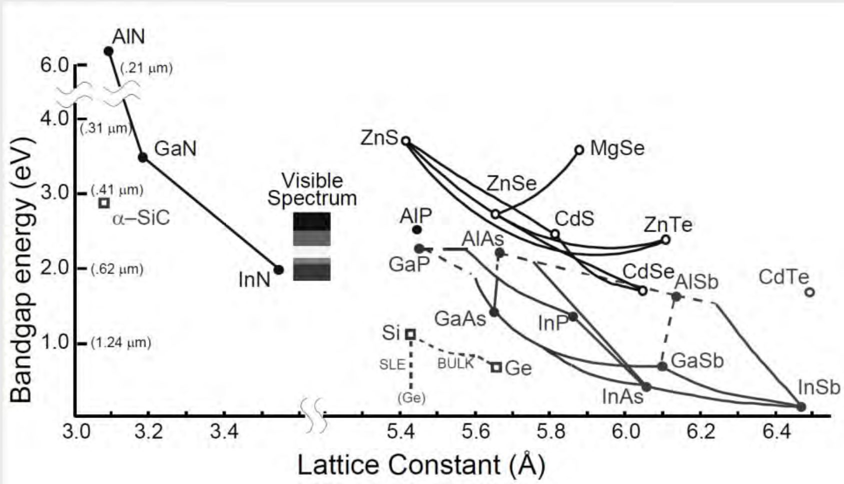

Mostly single or binary element (solid state chemists are way ahead!)
Silicon cannot emit light, but works as photodetectors (PDs)
Topological insulators and Weyl → spin selective PDs

NUS National University of Singapore

RRAM: random material breakdown
→ Stochastic

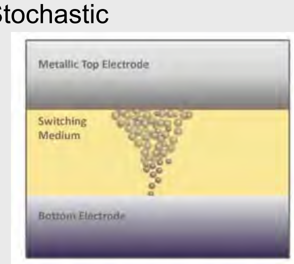

Figure 5: How it Works — In a switching media, nanoparticles form a conduction path between the top and bottom electrodes.
from Crossbar

FLASH: tunneling (writing)
→ Endurance issue (million cycles)

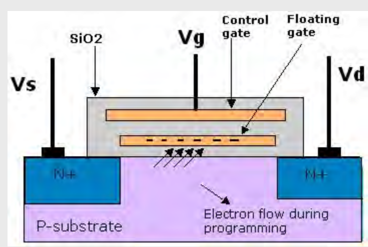

www.eeherald.com/

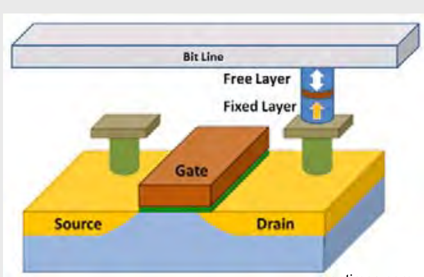

www.eetimes.com

MRAM: intrinsic material property
→ Deterministic

Spin transfer torque writing
→ Full selectivity
→ Smaller cell size

NUS National University of Singapore

Charge electronics → Spin electronics

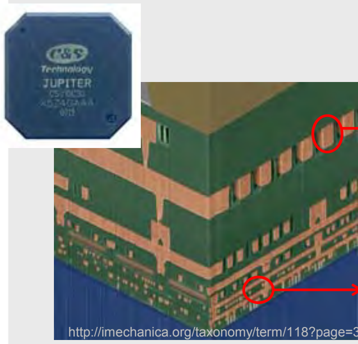

Information transfer
= electron transfer

Information processing
= processing electron flow

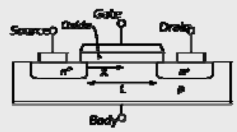

Spin wave interconnect

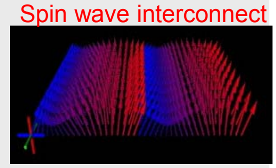

MTJ memory

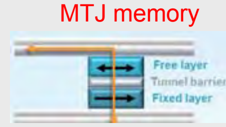

Spin transistor

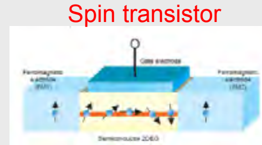

Charge transfer and processing energy loss is huge
→ All spin electronics

Spintronics

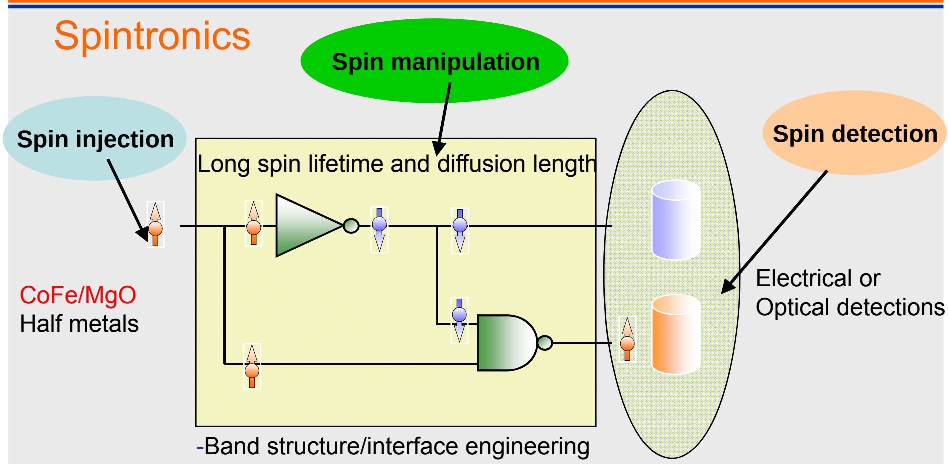

CoFe/MgO
Half metals

- Band structure/interface engineering
- Carbon nanotubes, graphenes
- Superconductors, nanodots
- Spin waves

Strong spin current generation → memory switching devices
Long spin lifetime (quantum computer), long spin diffusion length (information transfer)

MTJ read sensors in HDD

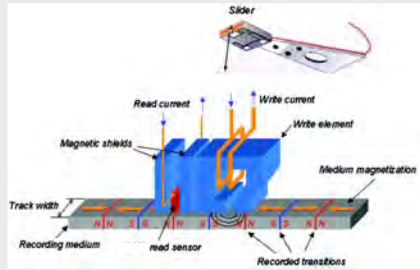

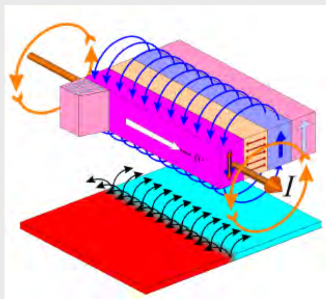

GMR ~ 10%
TMR ~ 50%

We understand MTJ sensor very well
Building high density MTJ array for MRAM is a different story

NUS National University of Singapore

20

Magnetic sensor applications

NUS National University of Singapore

24

Magnetic sensors in a car

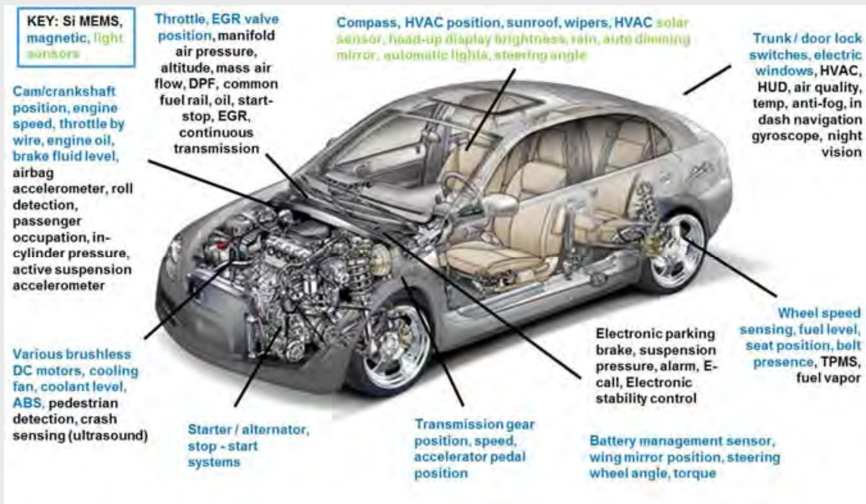

Graphene magnetic sensors

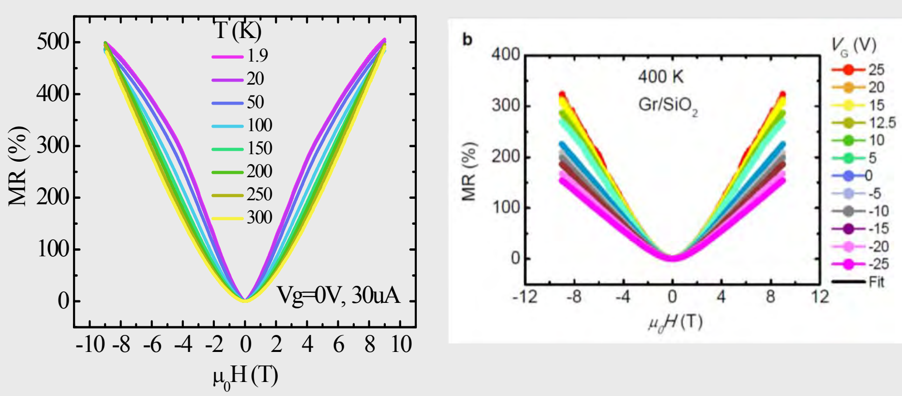

Temperature insensitive giant magneto-resistance (MR)
Gate tunable property
Giant MR is explained by inhomogeneous charge distribution

Phys. Rev. B **88**, 195429 (2013)

Systems showing linear MR

1. InSb Nat. Mater. 7, 697 (2008), Science **289**, 1530 (2000)
2. Ag_2Te and Ag_2Se Nature **390**, 57 (1997)
3. (Multilayer) graphene Nat. Comm. **6**, 8337 (2015), Phys. Rev. B 88, 195429 (2013) Nano Lett. **10**, 3962 (2010)
4. TI (Bi_2Se_3, Bi_2Te_3) APL **102**, 012102 (2013), PRL **108**, 266806 (2012)
5. Weyl-WTe_2 Nature **514**, 205 (2014)

Theoretical explanation of linear MR

- Classical model Nature **426**, 162 (2003)
- Quantum model PRB **58**, 2788 (1998)

28

Classical model

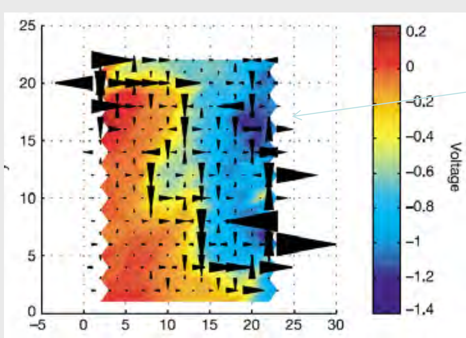

Inhomogeneity

Random resistor network

Local mobility fluctuations

Linear MR
(temperature independent)

Nature **426**, 162 (2003), Nature **477**, 304 (2011)

29

Quantum model

Low band-gap + small eff. mass

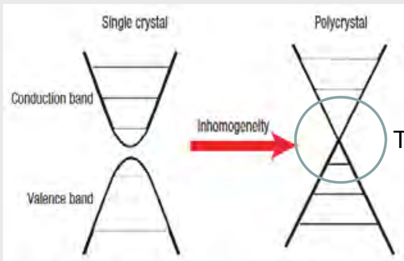

Inhomogeneity

↓ ħω > E_F

Tail formation

↓

Linear E-k

↓

Linear MR
(temperature independent)

$$\rho_{xx} = \rho_{yy} = \frac{N_i H}{\pi n^2 e c}$$

Abrikosov, A. A. Quantum magnetoresistance. Physical Review B **58**, 2788 (1998)

Two channel model

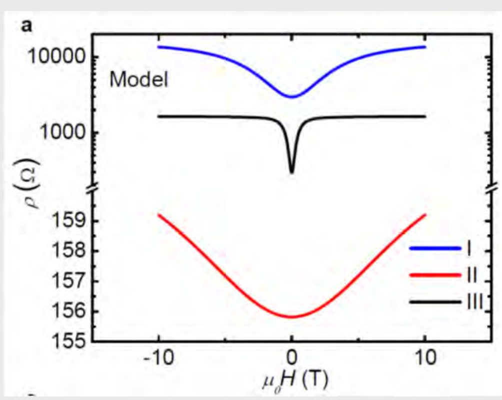

High sensitivity at low field
is important for applications

$$MR_\infty \approx \frac{n_1 n_2}{(n_1+n_2)^2}\frac{\mu_1}{\mu_2} >> 1$$

Case I	$n_1=10^{11}$ cm^{-2}, $n_2=1.1\times10^{11}$ cm^{-2}, μ_1=20,000 cm^2 V^{-1} s^{-1}, μ_2=1,000 cm^2 V^{-1} s^{-1}
Case II	$n_1=8\times10^{12}$ cm^{-2}, $n_2=1.1\times10^{11}$ cm^{-2}, μ_1=5,000 cm^2 V^{-1} s^{-1}, μ_2=1,000 cm^2 V^{-1} s^{-1}
Case III	$n_1=10^{11}$ cm^{-2}, $n_2=1.1\times10^{11}$ cm^{-2}, μ_1=200,000 cm^2 V^{-1} s^{-1}, μ_2=10,000 cm^2 V^{-1} s^{-1}.

Large mobility difference is important for a large MR

Nat. Comm. **6**, 8337 (2015)

BN/graphene heterostructures

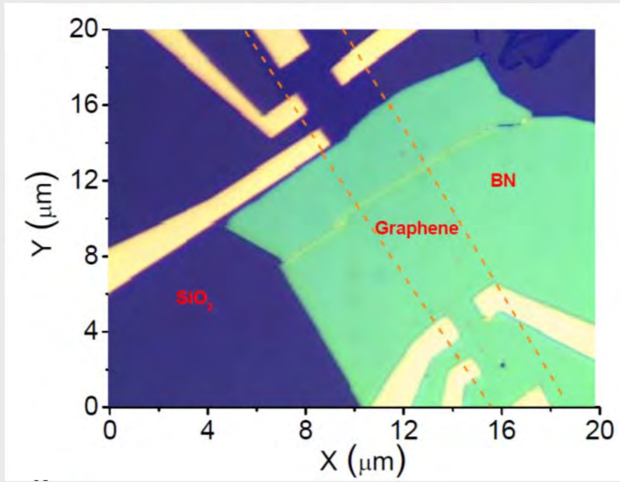

- Boron nitride (BN)/graphene heterostructures can provide a big mobility difference

Nat. Comm. **6**, 8337 (2015)

39

Giant MR from BN/graphene heterostructures

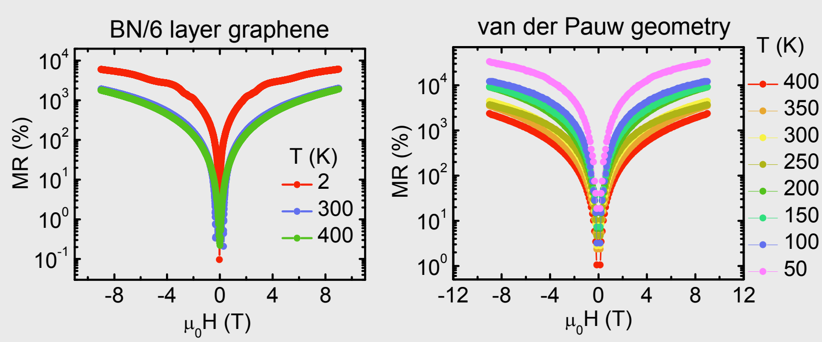

BN/6 layer graphene → Giant local MR of 2000% at 400 K
van der Pauw geometry → 35,000% at 50 K

Nat. Comm. **6**, 8337 (2015)

42

Non-local MR

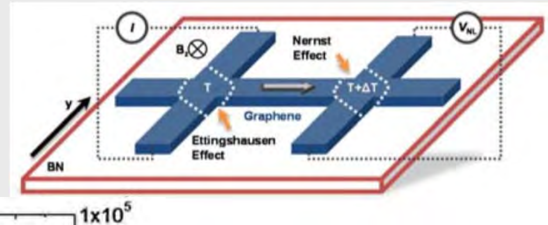

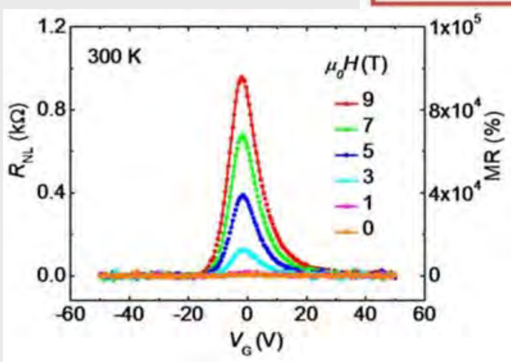

4 layer graphene/BN at 300 K

non-local MR value of 90,000%

Ettingshausen-Nernst effect

Nat. Comm. **6**, 8337 (2015)

43

Graphene applications

A roadmap for graphene

K. S. Novoselov, V. I. Fal'ko, L. Colombo, P. R. Gellert, M. G. Schwab & K. Kim

192 | NATURE | VOL 490 | 11 OCTOBER 2012

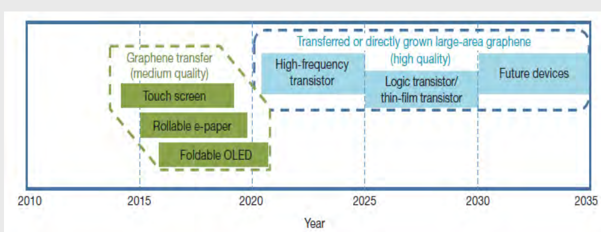

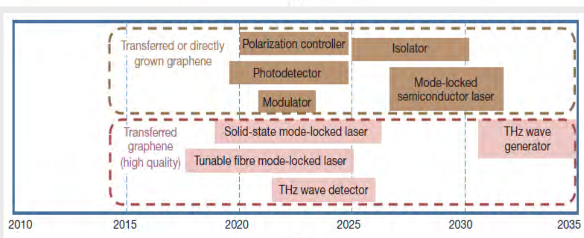

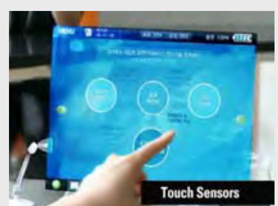

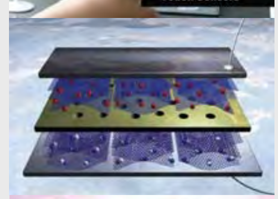

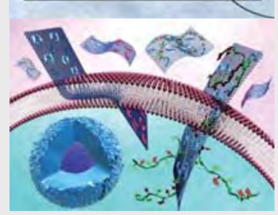

THz

44

Applications of Terahertz Light

Stand-off detection of hidden objects and weapons

Safe, non invasive and quick imaging through different types of clothing, concealments and other confusion materials.

Non-invasive medical and dental diagnostics

High-sensitivity, safe detection of cancerous tissue and dental caries for earlier and more accurate diagnosis.

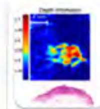

Drug discovery and formulation analysis of coatings and cores

In-line control of pharmaceutical products for better understanding of product and process design.

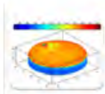

Characterisation of electron carriers and metamaterials

Improving the performance and quality of solid-state properties of semiconductors and metamaterials.

Non-contact material integrity imaging of coatings and composites

Imaging of coating layers on metal and polymer automotive structures to identify presence of defects in paints.

Non-destructive rapid fault isolation in IC packages

High-accuracy isolation of shorts, dead opens, and resistive opens for localising defects in complex packages.

Detection of cracks and defects in solar panels

Inspection and quality control of crucible coatings, silicon and thin films cracks and defects in solar panels.

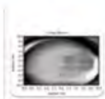

Non-contact imaging for conservation of paintings, manuscripts and artefacts

Perform spectroscopic analysis without any contact with valuable and delicate paintings and artefacts.

http://www.teraview.com/applications/

NUS National University of Singapore

55

Giant THz machine

-We need to miniaturize big THz machine.
-For this we need various small THz devices,
such as phase shifters, modulators, generators, etc.

NUS National University of Singapore

56

Problems in conventional THz phase shifters

Bulky magnets required | High voltage (200 V) required

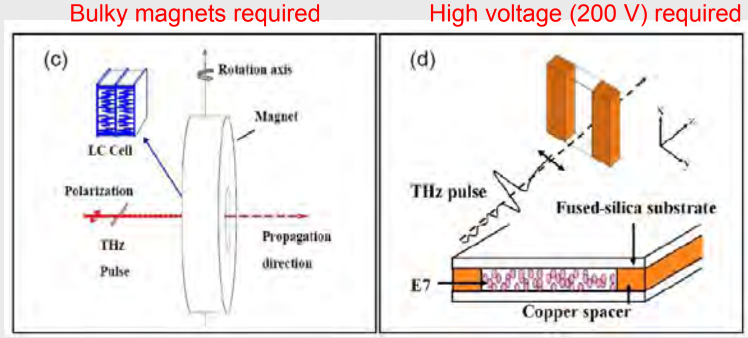

Chen C. Y. *et al.* Magnetically tunable room-temperature 2π liquid crystal terahertz phase shifter. Optical Express. **(2004)**

Hsieh C. F. *et al.* Voltage-controlled liquid-crystal terahertz phase shifter and quarter-wave plate. Optical Letters. **(2006)**

57

Schematic diagram of the THz phase shifters

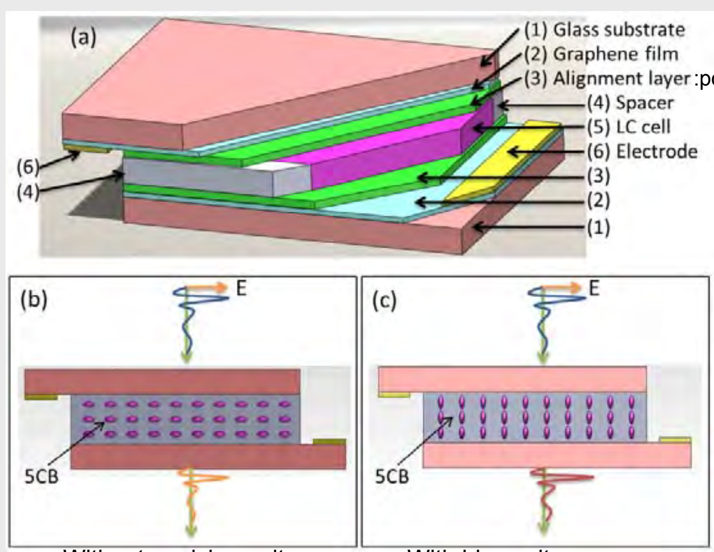

Without applying voltage | With bias voltage

Optics Express **21**, 21395 (2013)

58

Transmittance of ITO vs. graphene

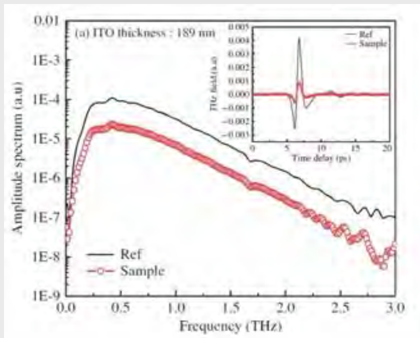

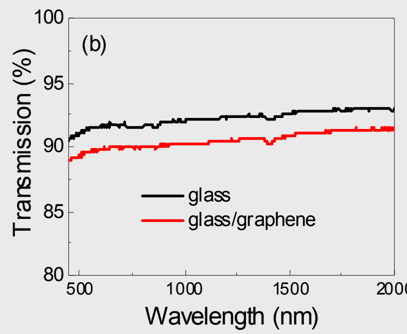

Ching-Wei Chen, *et al.* IEEE Journal of Quantum Electronics (2010)

Transparency of ITO films is poor at THz frequencies
ITO : < 10% transmission at 0.2 -1.2 THz

Graphene: ~98% transmission in visible & NIR
How about in THz?

NUS National University of Singapore

59

Transparency of CVD graphene at THz

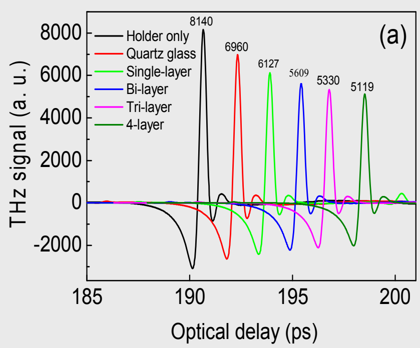

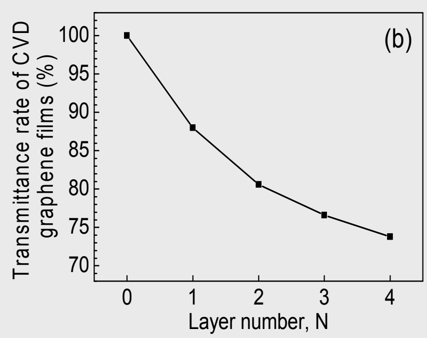

Pulses are shifted for clarify

-Excellent transmission in THz
-Non-linear transmittance decay
-Uniform absorption within 0.5 – 4 THz

NUS National University of Singapore

Optics Express **21**, 21395 (2013)

60

THz phase shift measurements

THz time delay under different bias voltages

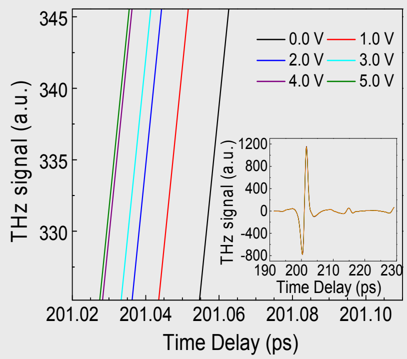

Voltage controlled phase shifts

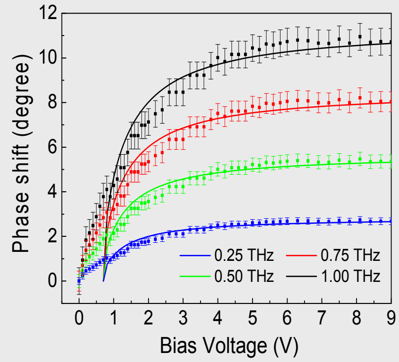

Low bias voltage operation (~ 5 V for saturation).
Linear controllability in low bias voltages.

Optics Express **21**, 21395 (2013)

Graphen/ionic liquid THz modulation

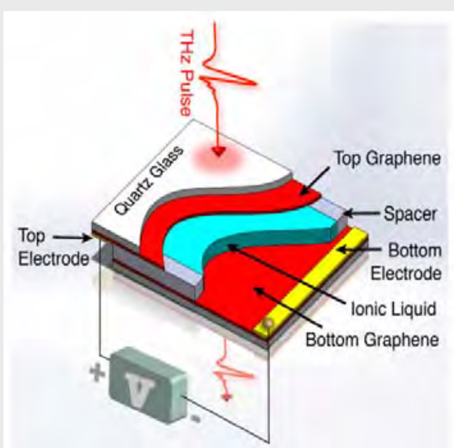

Utilizing intra-band absorption

$$\sigma(\omega) = \sigma_{DC}(E_F)/(1+\omega^2\tau^2)$$

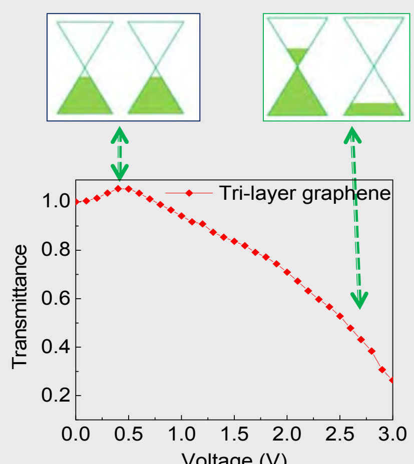

Adv. Mat. **27**, 1874 (2015)

Geometry & layer thickness dependence study

Modulators with 50 µm & 100 µm ionic liquid cells

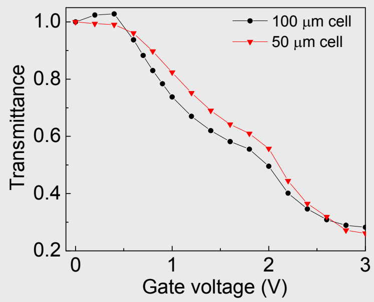

Similar modulation depth for devices with different cell thickness

Multilayer & double-deck modulators

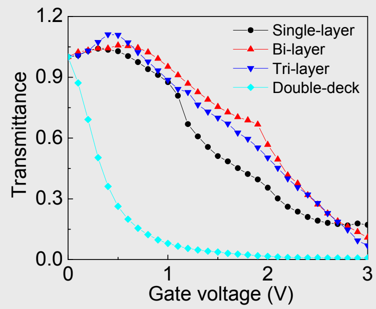

Transmittance

- Mono-layer 83%
- Bi-layer 89%
- Tri-layer 93%
- Double deck 99%

Adv. Mat. **27**, 1874 (2015)

Logic device (switch) applications

For switch applications, on/off current ratio should be

(TFT panel) > 100, Conventional logic CMOS > 1000

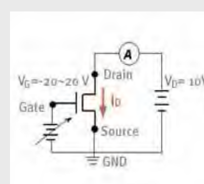

Need to increase TMR (→Need a high spin polarization)

$$MR = \frac{R_{AP} - R_P}{R_P} = \frac{2P_1P_2}{1 - P_1P_2}$$

New material for electrodes and barriers

- MgO spin filter (on/off ration < 10)
- Half metals (only at low temp.)

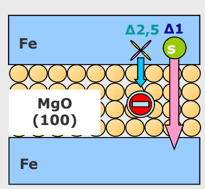

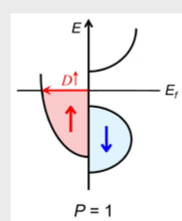

Almost perfect switches/filters → nonreciprocity

Mechanical switch

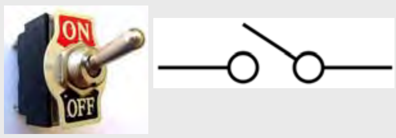

Transistor

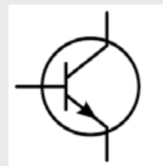

Optical filter

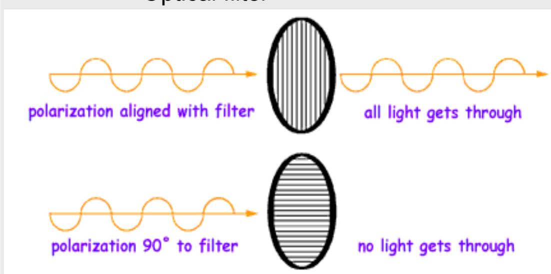

Microwave circulator

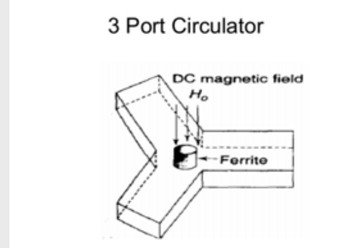

Is there any similar component in spintronics?

NUS National University of Singapore

76

Describing spin waves

Single electron spin

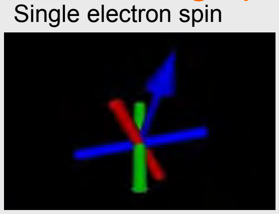

1D chain of (dipolar/exchange) coupled electrons

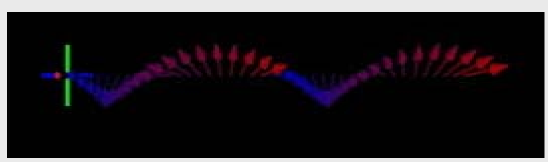

Collective magnetization dynamics: spin waves

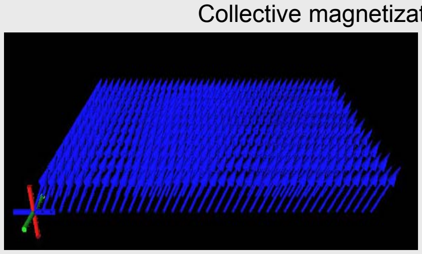

FMR
Uniform precession (standing waves)

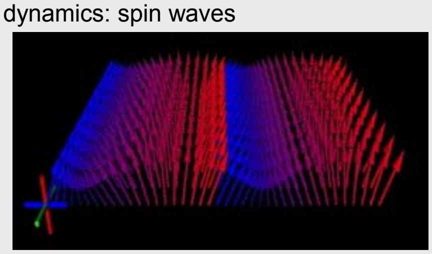

Spin waves
Travelling waves

NUS National University of Singapore

77

Measurements set-up and layer structure of spin wave device

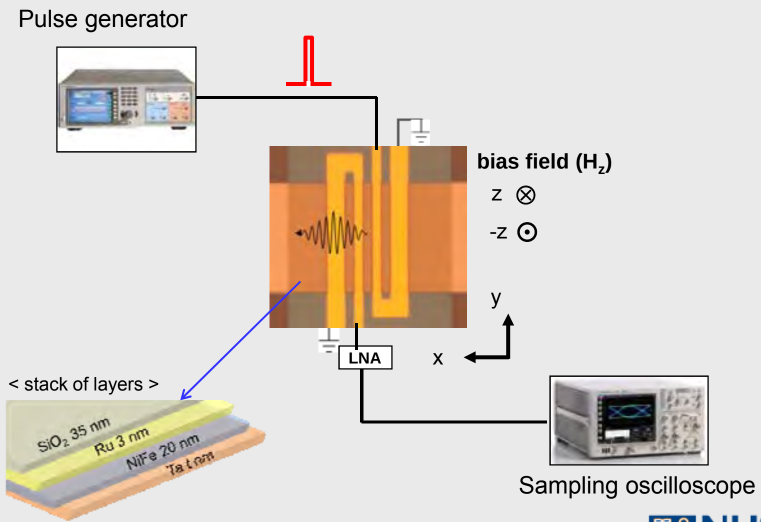

t_{Ta} (Ta thickness) ranges from 0 to 10 nm

Giant nonreciprocal emission of spin wave in Ta/Py

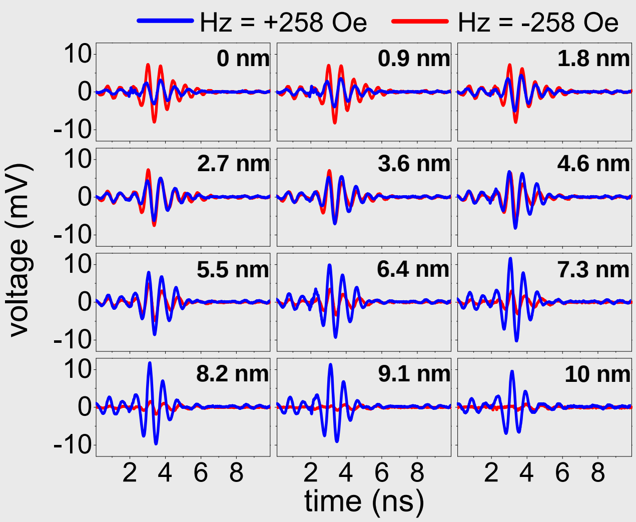

ON / OFF ratio of 60

- The amplitude at -258 Oe is higher than that at +258 Oe in the device for $0 < t_{Ta} < 2.7$ nm.
- However, the amplitude at +258 Oe is higher than that at -258 Oe for $4.6 \text{ nm} < t_{Ta} < 10$ nm

Giant nonreciprocity due to spin pumping

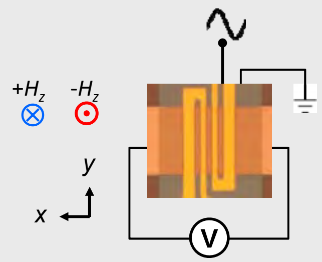

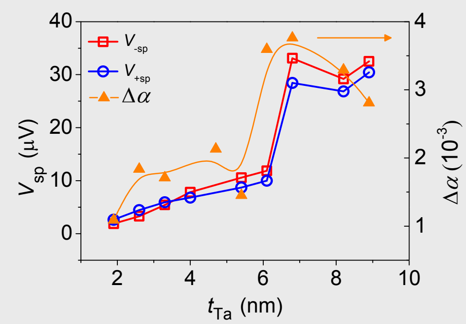

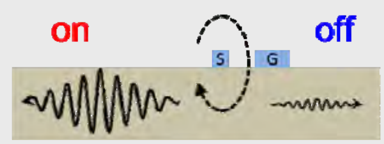

Hall effect & spin Hall effect (SHE)

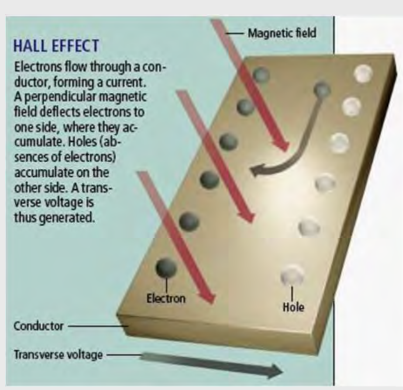

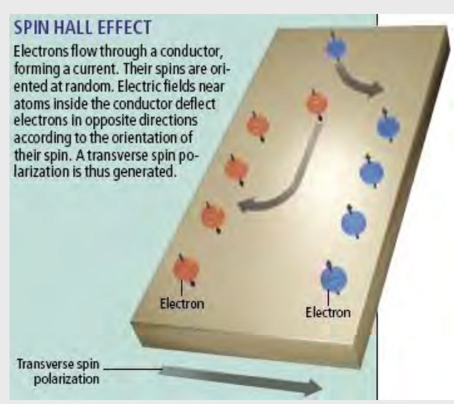

SHE: Separate electrons of different spins without using a magnetic field

Y.K. Kato, Sci. Am. 2007

Spin-orbit torques (SOT)

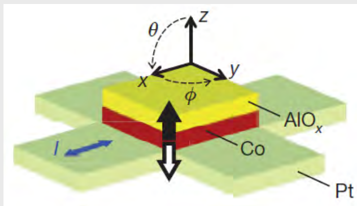

Miron *et al*. Nature **476**, 189 (2011)

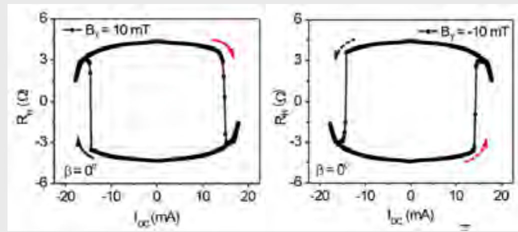

Liu *et al.* PRL **109**, 096602 (2012)

- Heavy metal/ferromagnetic material/oxide layer.
- Current induced magnetization switching is observed (longitudinal field needed).
- Magnetization states depend on both current and field directions.
- Possible mechanisms: Rashba effect & spin Hall effect (SHE).

83

Perpendicularly magnetized trilayer structures

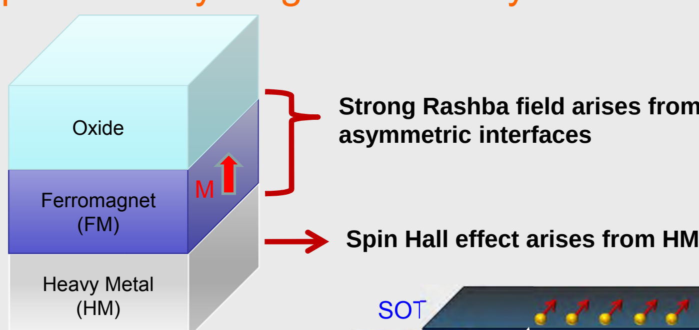

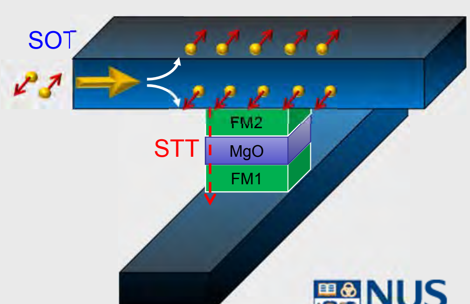

In-plane currents can switch the magnetization

85

Spin Hall angle (θ_{SH})

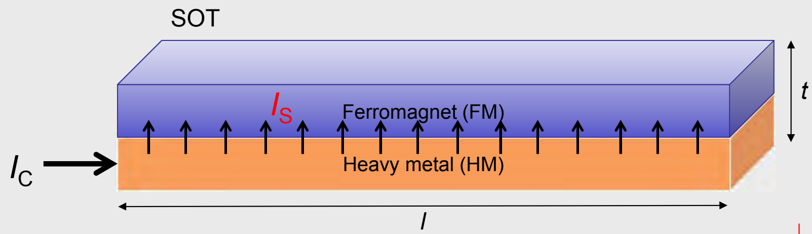

$$\frac{I_S}{I_C} = \theta_{SH} \frac{l}{t} (\theta_{SH} = \frac{\sigma_S}{\sigma_c})$$

$l >> t$

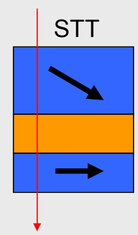

Spin currents can be very large, as the electron can interact with the FM many times (lateral scattering)

87

Spin Hall angle is a material parameter

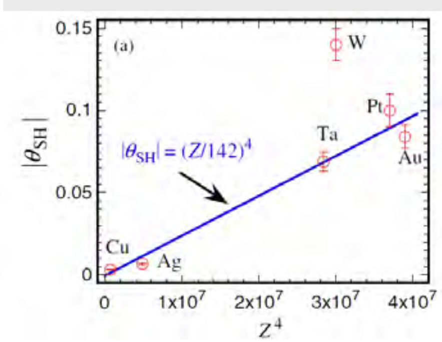

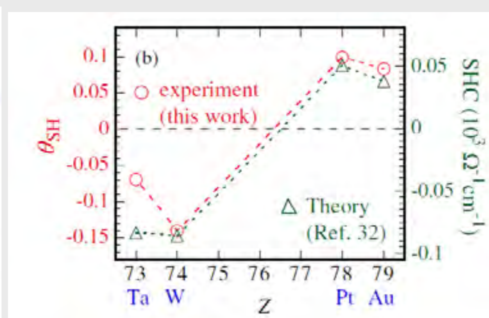

Number of d-electrons

Luckily some CMOS compatible materials show large spin Hall angles.

PRL **112**, 197201 (2014), Phys. Rev. B **77**, 165117 (2008), Phys. Rev. B **83**, 174405 (2011)

Heavy Weyl semimetals → strong spin orbit coupling

88

Various reported θ_{SH} in Pt

Is it a constant value for a given material?

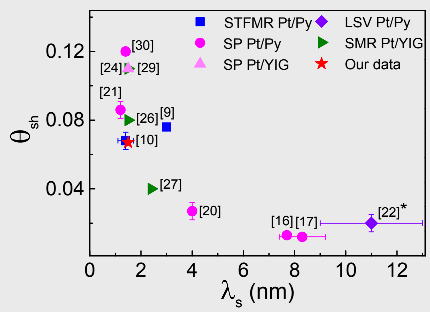

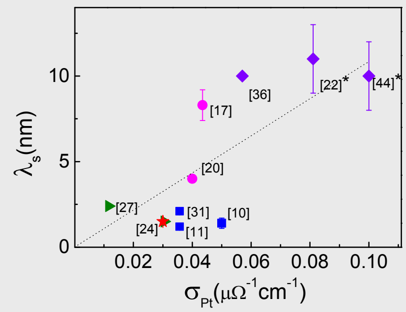

- Relationship of $\theta_{SH}\lambda_S$ ~ 0.13 nm & $\lambda_S \propto \sigma_{Pt}$
- Can we engineer θ_{SH} by changing σ_{Pt}?

APL 105, 152412 (2014)

89

Spin Hall angle engineering

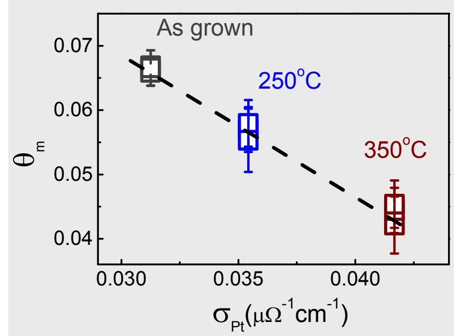

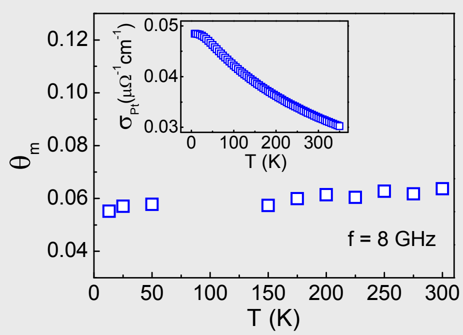

- Annealing condition can change θ_{SH} for the same material.
- Dominant mechanism for θ_{SH} in Pt is not intrinsic.
- Can we increase θ_{SH}?

APL 105, 152412 (2014)

90

Spin Hall vs. interfacial Rashba

Reverse switching polarity by oxygen engineering

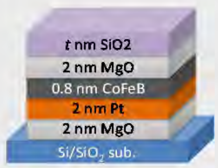

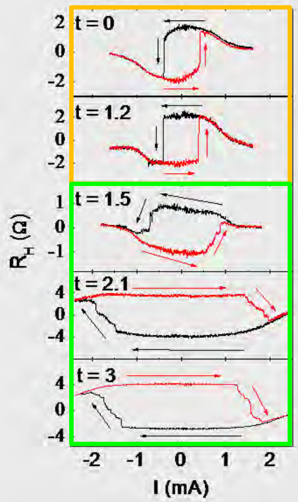

$\theta_{SH} < 0$

$\theta_{SH} > 0$

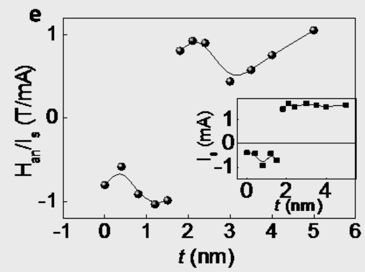

-Sign of spin Hall angle changes across a transition thickness of SiO_2 (*t* = 1.5 nm)
-Cannot understand by spin Hall physics → suggest the role of interface

Nat. Nanotech. **10**, 333 (2015)

Spin-orbit torque switching currents

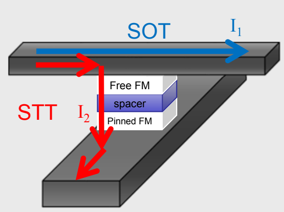

$$I_c \approx \frac{2e}{\hbar}\left(\frac{\alpha M_S V}{\eta P}\right) H_{eff} \quad \text{STT}$$

$$I_c \approx \frac{e}{\hbar}\left(\frac{M_S t_{FM} A_{HM}}{\theta_{SH}}\right) H_{eff} \quad \text{SOT}$$

K.J.Lee, APL (2013)

-No damping term → great flexibility for choosing FM, high speed

-No spin polarization term → no need to use MgO

-Can use thick MgO→ eliminate MgO breakdown issue

-Large spin Hall angle (θ_{SH}) or effective field (H_{eff}) is the key

$H_{eff} = \hbar\theta_{SH}|j_e|/(2|e|M_S t_F)$

NUS National University of Singapore

Large spin Hall angles from various materials

FePt/Au spin Hall angle (θ_{SH}) = 0.1 (Takanashi group)

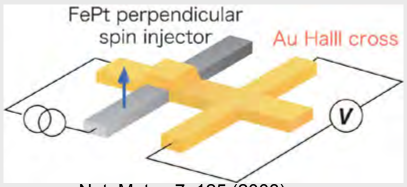

Nat. Mater. 7, 125 (2008)

CuBi θ_{SH} = -0.24 (Otani group)

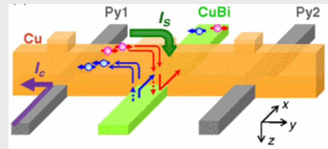

Phys. Rev. Lett. 109, 156602 (2012)

Co/Pd multilayer θ_{SH} = 4 (NUS)

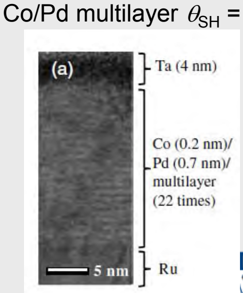

β-W θ_{SH} = 0.3 (Cornell)

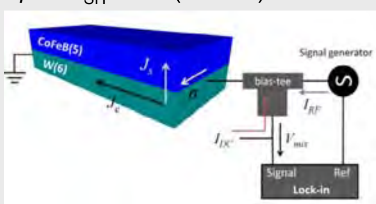

Appl. Phys. Lett. 101, 122404 (2012)

Phys. Rev. Lett. **111**, 246602 (2013)

Spin orbit torques in Co/Pd multilayers

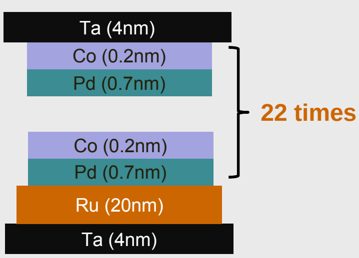

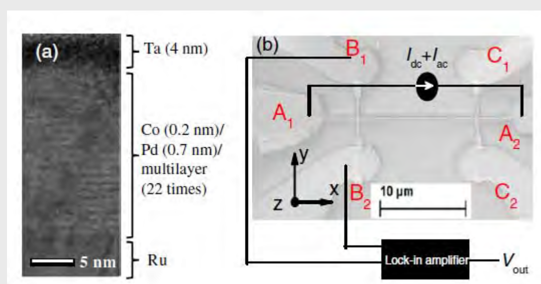

TABLE I. Summary of the reported longitudinal and transverse torque components and the extracted dimensionless coefficients. The values in the brackets indicate the corresponding effective efficiency $\alpha_{\parallel,\perp}$. For the present work we used $t = 20$ nm and $M_S = 6.23 \times 10^5$ A/m. Note that the torques from Ref. [27] are taken at $\theta = 0$.

Structure (nm)	$\beta_{\parallel}$ (Oe/10^8 A/cm^2) [$\alpha_{\parallel}$]	$\beta_{\perp}$(Oe/10^8 A/cm^2) [$\alpha_{\perp}$]	$\beta_{\perp}/\beta_{\parallel}$	Ref.
Ta(4)/$Co_{40}Fe_{40}B_{20}$(1)/MgO(1.6)	350 [0.12]	-		[6]
Ta(3)/$Co_{40}Fe_{40}B_{20}$(0.9)/MgO(2)	240 [0.07]	450 [0.13]	1.9	[27]
Ta(1.5)/$Co_{40}Fe_{40}B_{20}$(1)/MgO(1.6)	135 [0.078]	472 [0.27]	4	[10]
Pt(3)/Co(0.6)/AlO_x(1.6)	690 [0.13]	400 [0.073]	0.58	[27]
Ta(4)/Ru(20)/$(Co/Pd)_{22}$/Ta(4)	1170 [4.4]	5025 [19.1]	4.3	This work

Phys. Rev. Lett. **111**, 246602 (2013)

Structural asymmetry can be added up

TEM data

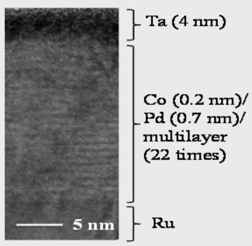

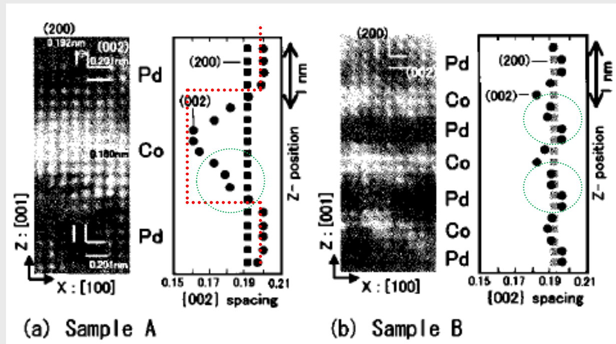

Maesaka, IEEE Trans. Magn. 38, 2676 (2002)

-Two successive Co/Pd and Pd/Co interfaces are structurally dissimilar.

-Lattice mismatch (9%) between Pd and Co

Phys. Rev. Lett. **111**, 246602 (2013)

113

LAO/STO – 2DEG formation

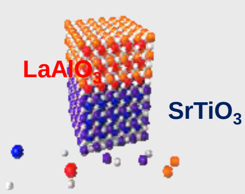

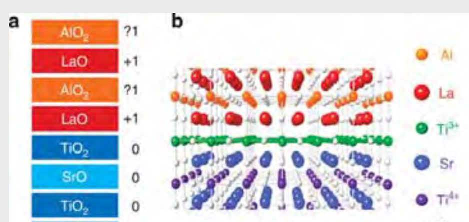

Nat. Comm. 4:1838

$LaAlO_3$ grown on TiO_2 terminated $SrTiO_3$ (100)

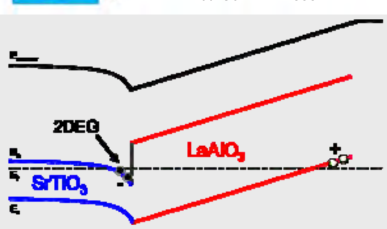

- ❑ $SrTiO_3$ (Insulator 3.2 eV)
- ❑ $LaAlO_3$ (Insulator 5.6 eV)

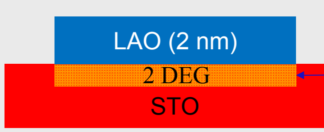

2 DEG formed inside the STO side

114

Magnetism in $LaAlO_3/SrTiO_3$ heterostructures

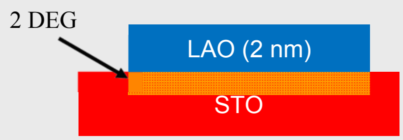

In-plane angular measurements

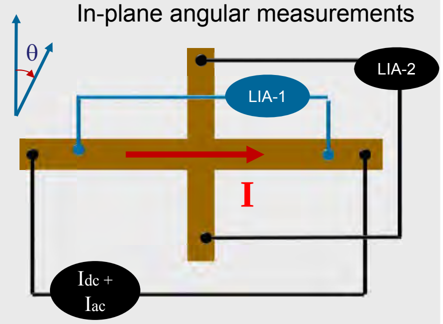

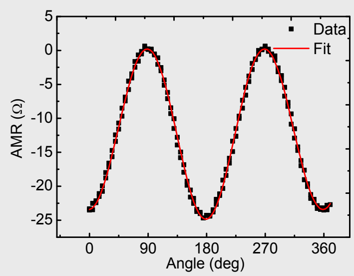

AMR measurements at $H = 9$ T , $T = 4$ K

$$R_{XX} = a_0+a_1\cos^2(\theta+\phi) + a_2\cos^4(\theta+\phi)$$

a_0, a_1, a_2 are constants

Appl. Phys. Lett. 105, 162405 (2014)

116

Asymmetric spin-orbit fields

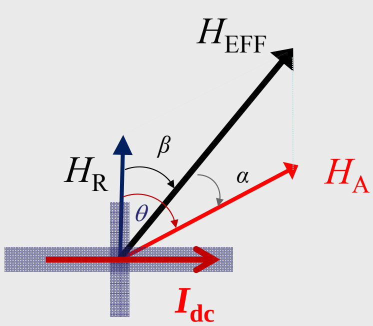

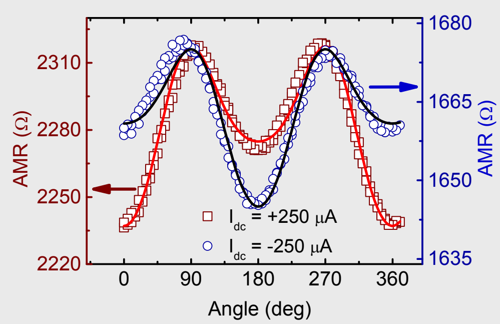

$$H_{EFF}^2 = H_A^2 + H_R^2 + 2H_A H_R \cos\theta$$

$$R_{XX} = b_0 + b_1 H_{EFF} \cos^2\alpha + b_2 H_{EFF} \cos^4\alpha$$

$H_R(+I)$ = 1.26 T
$H_R(-I)$ = -1.48 T

H_R, H_A H_{EFF} are Rashba, applied and effective fields

b_0, b_1, b_2 are constants

Appl. Phys. Lett. 105, 162405 (2014)

117

Current induced spin-orbit fields in 2DEG

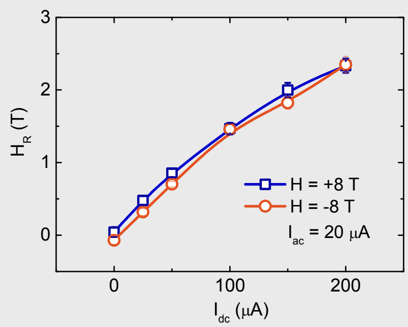

Assuming thickness of 2DEG
t_{2DEG} = 7 nm
Nat. Mater. **7**, 621 (2008)

current density = 7.14×10⁸ A/m²

2.35 T @ 200 μA
→ **32.9** Tesla/10⁶ A/cm²

The highest current induced torque reported in metallic system is only 0.5 T.

PRL **111**, 246602 (2013)

$\alpha_R = \sqrt{\hbar^3 e H_{so} / m^{*2}}$ H_{so} = 1.48 T, α_R = 12 meV·Å, spin splitting Δ = 3 meV (~30 T)

cf. Co/Pd multilayer α_R =360 meV·Å

Appl. Phys. Lett. 105, 162405 (2014)

NUS National University of Singapore

118

Topological insulators (TIs)

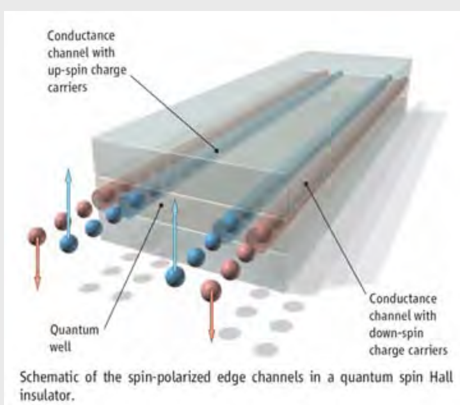

Schematic of the spin-polarized edge channels in a quantum spin Hall insulator.

Nobel Symposium 2010, Shoucheng Zhang

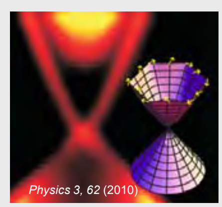

ARPES spectra showing a linear band structure of the surface states on a 3D TI

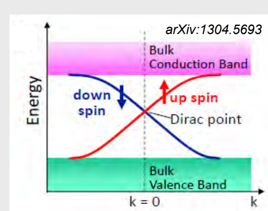

- ❑ Linear dispersion
- ❑ Spin polarized surface currents
- ❑ Spin-momentum locking → giant spin Hall angle ?

NUS National University of Singapore

147

BiSbTeSe$_2$ topological insulators

Can TI survive after etching process?

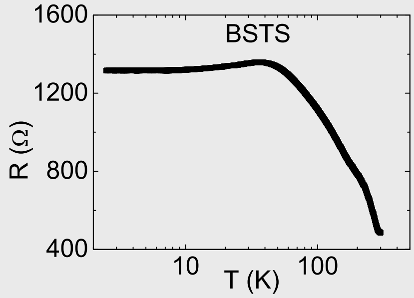

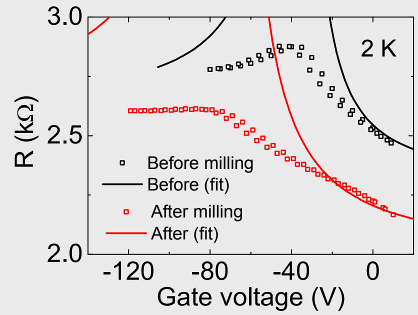

BiSbTeSe$_2$ is semiconducting

Sample has become more heavily n-doped after ion milling

-Charged impurity density(n_{imp}): $7 \times 10^{12} \rightarrow 1.33 \times 10^{13}$/cm^2
-Carrier concentration: 2.36×10^{13} /cm^2 $\rightarrow$ 5.53×10^{13} /cm^2
-Mobility (μ_e): 106 $\rightarrow$ 52 cm^2/(V·s)

NUS National University of Singapore

Phys. Rev. B, **90**, 235427 (2014)

148

Ar ion milling effects

[BiSbTeSe (1.5-0.5-1.8-1.2)]

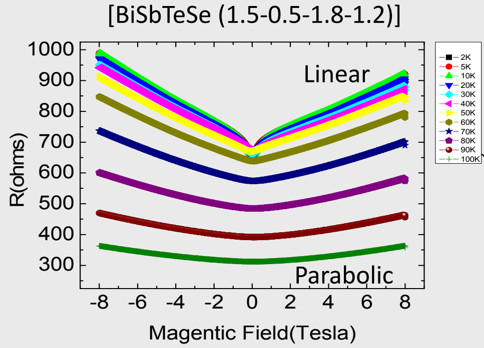

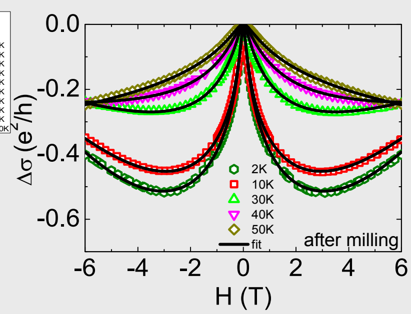

Linear MR at LT
Parabolic MR at RT

Negative MR originates from disorder

NUS National University of Singapore

Phys. Rev. B, **90**, 235427 (2014)

149

Robustness of the topological surface states

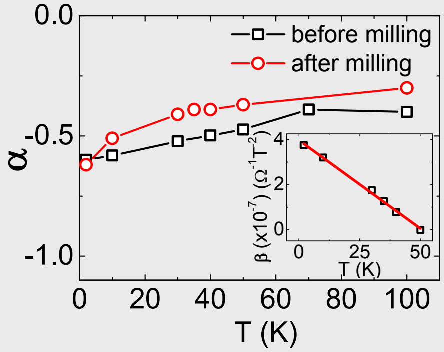

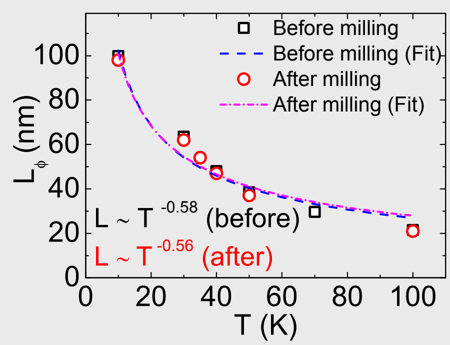

-A decay constant of -0.5 in L_ϕ indicates two-dimensional (2D) electron-electron scattering for the sample before and after milling.
-The behavior of surface states is unaffected by the introduction of disorder, as inferred from the similar values of α and the behavior of L_ϕ.
-Surface states are remarkably robust against external damage induced by ion milling.

NUS National University of Singapore

Phys. Rev. B, **90**, 235427 (2014)

Experimental setup

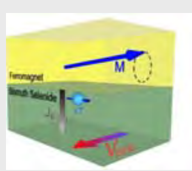

Magnetization oscillation provides high density spin currents into TI and a transverse voltage is detected in TI spin detector.

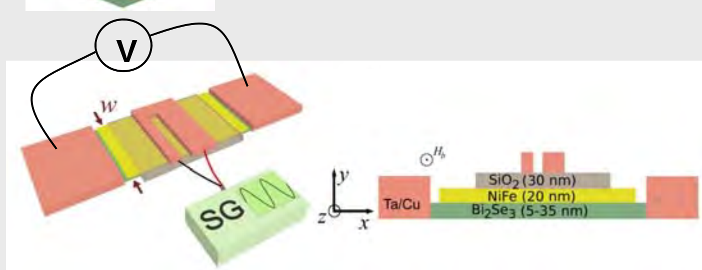

- Signal generator to excite magnetization dynamics in NiFe through a coplanar waveguide
- Voltmeter to measure spin pumping induced ISHE
- Vector network analyzer for FMR measurements

NUS National University of Singapore

Phys. Rev. B **90**, 094403 (2014)

ISHE measurements

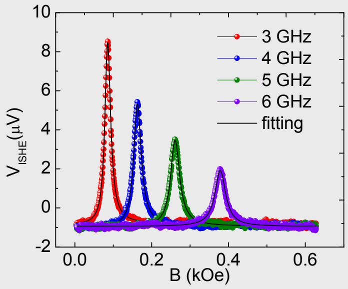

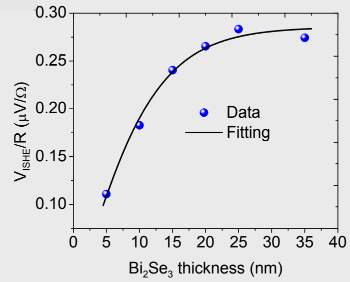

$V_{ISHE} \sim R \cdot J_s \cdot \theta_{SH}$

$$\frac{V_{ISHE}}{R} = \theta_{sh} w d_{BiSe} \left(\frac{2e}{\hbar}\right) \frac{\hbar g_{r\uparrow\downarrow} \gamma^2 h_{rf}^2 \left(M\gamma + \sqrt{M^2\gamma^2 + 4\omega^2}\right)}{8\pi\alpha^2 \left(M^2\gamma^2 + 4\omega^2\right)} \frac{\lambda_{sf}}{d_{BiSe}} \tanh\left(\frac{d_{BiSe}}{2\lambda_{sf}}\right)$$

R is resistance of the film
J_s is induced spin current
θ_{SH} is spin Hall angle

⇨ $\theta_{sh} = 0.01$
$\lambda_{sf} = 6.2$ nm

NUS National University of Singapore

Phys. Rev. B **90**, 094403 (2014)

157

Extracted spin Hall angle

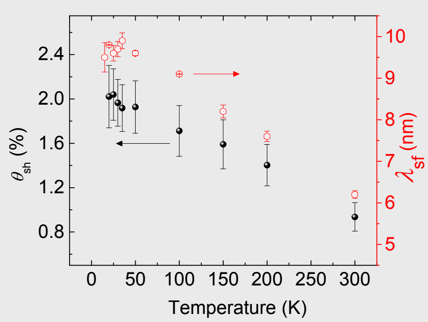

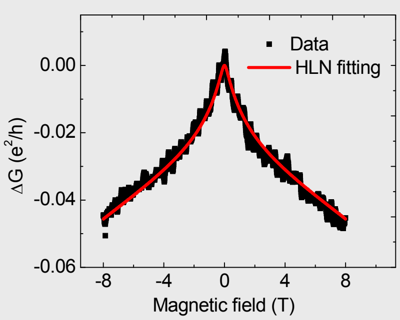

Spin orbit length, l_{so} = 6.9 nm

- 1-2% of spin Hall angle is identified, which is already comparable to the best data from heavy metals (Pt, Ta).
- $l_{so} \sim \lambda_{sf}$ suggest that spin-orbit coupling is dominant source of spin scattering

NUS National University of Singapore

Phys. Rev. B **90**, 094403 (2014)

161

No spin momentum locking

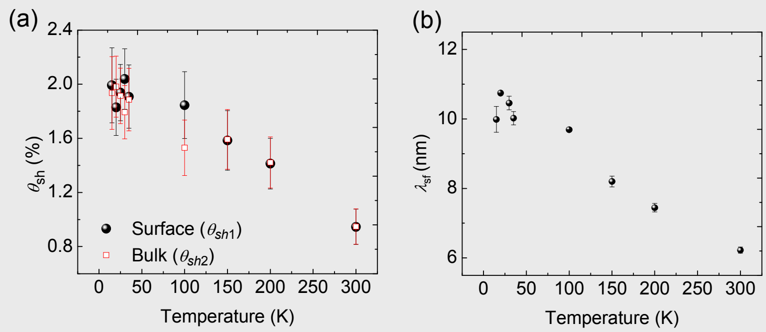

- Assumed spin Hall angle at opposite surfaces was taken to be of opposite signs.
- Spin Hall angle does not show any clear distinction between the surface and bulk value
- Momentum locking signature is not detected.

Phys. Rev. B **90**, 094403 (2014)

Comparison with other reports

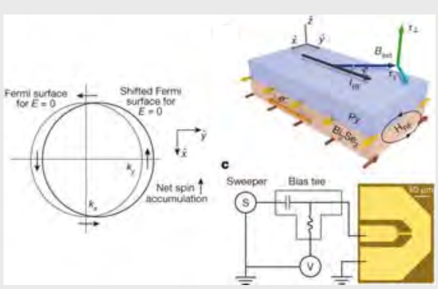

Nature **511**, 449 (2014)

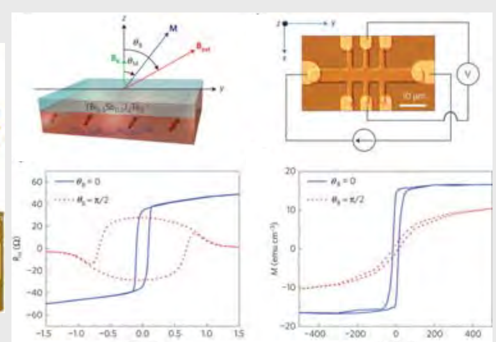

Nat. Mater. **13**, 699 (2014)

Spin torque ferromagnetic resonance measurements ➔ θ_{SH} = 2.0 – 3.5

Magnetization switching by current induced spin orbit torque ➔ θ_{SH} = 140 – 425

In these experiments, a charge current flows through the TI material, unlike ours.

ST-FMR measurement of Bi_2Se_3/CoFeB

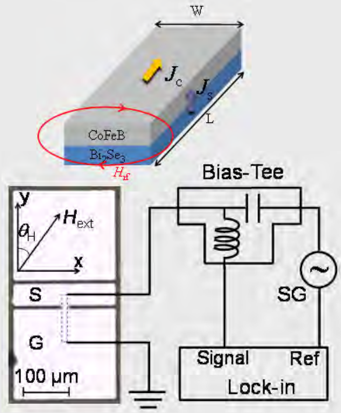

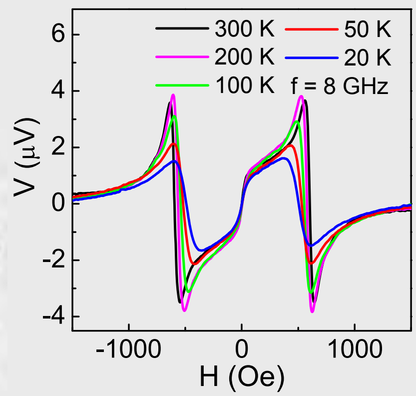

- ST-FMR measurements with a lock-in amplifier at θ_H = 35°.
- ST-FMR signal (V_{mix}) can be fitted by a sum of symmetric and antisymmetric Lorentzian functions:

$$V_{mix} = V_s F_{sym}(H_{ext}) + V_a F_{asym}(H_{ext})$$

V_s: in-plane torque $\tau_{||}$ on CFB
V_a: total out-of-plane torque

NUS National University of Singapore

PRL **114**, 257202 (2015)

167

In-plane spin-orbit torque ratio in Bi_2Se_3/CoFeB

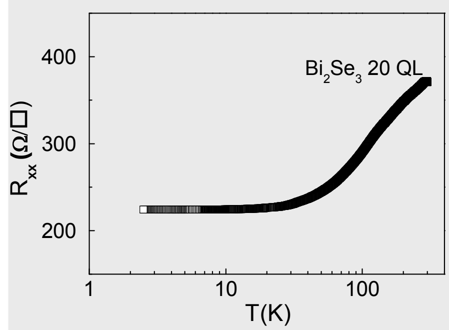

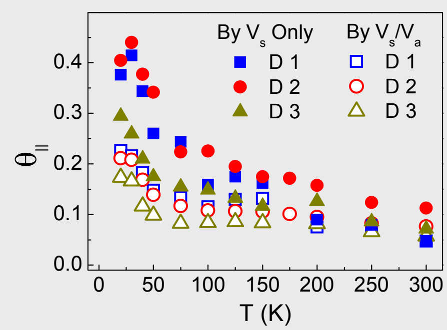

- $\tau_{||}$ ($\theta_{||}$) increases steeply and nonlinearly to **~ 0.42** at low temperature and could be almost 10 times larger than that at 300 K.
- The polarization direction of $\tau_{||}$ is consistent with spin-momentum-locked TSS.
- $\theta_{||}$ by 1st and 2nd methods shows a significant difference below ~ 50 K, other out-of-plane torque may contribution besides τ_{Oe}.

NUS National University of Singapore

Wang *et al.*, PRL **114**, 257202 (2015)

170

Out-of-plane spin-orbit torque ratio in Bi_2Se_3/CoFeB

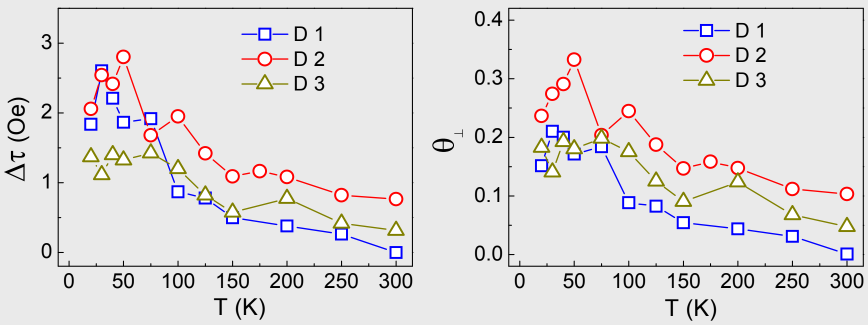

- ❑ $\Delta\tau\,(\theta_{\perp})$ also increases at low temperature similar to $\tau_{||}\,(\theta_{||})$.
- ❑ Rashba-split state in 2DEG of Bi_2Se_3 is not the main mechanism for $\Delta\tau$.
- ❑ Hexagonal warping in the TSS of Bi_2Se_3 can account for $\Delta\tau\,(\theta_{\perp})$.

Wang *et al.*, PRL **114**, 257202 (2015)

Out-of-plane torque in Bi_2Se_3

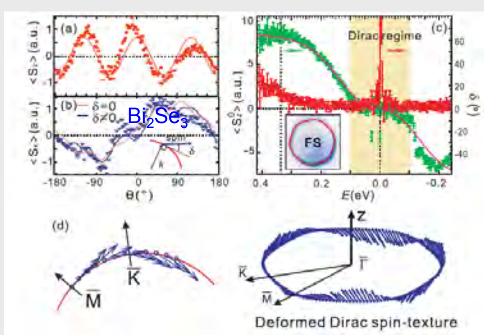

Wang *et al.*, PRL **107**, 207602 (2011)

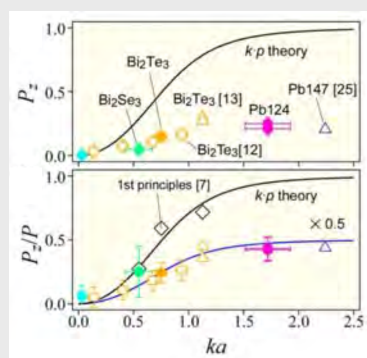

Nomura *et al.*, PRB **89**, 045134 (2014)

-Recent reports showed there is substantial out-of-plane spin polarization due to Hexagonal warping.

-**Hexagonal warping** in the TSS of Bi_2Se_3 can account for $\Delta\tau\,(\theta_{\perp})$.

Estimation of $\theta_{||}$ from topological surface states (TSS)

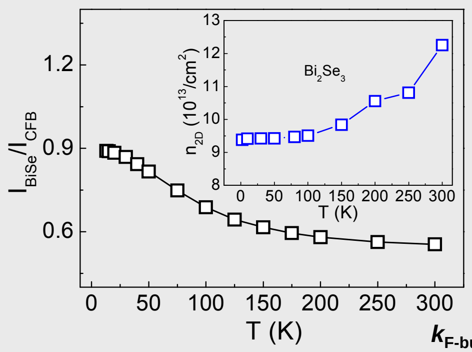

$k_{F\text{-}TSS}$ ~ 0.14 – 0.17 Å^{-1}
$k_{F\text{-}2DEG}$ ~ 0.1 – 0.12 Å^{-1}
$n_{2D} = 2n_{TSS} + 2n_{2DEG} + n_{bulk}d$
n_{TSS} ~ 1.56 − 2.3×10^{13} cm^{-2}
n_{2DEG} ~ 1.59 − 2.3×10^{13} cm^{-2}
n_{bulk} ~ 1 − 3.1×10^{19} cm^{-3}
(~ 1 − 3.1×10^{13} cm^{-2})
$k_{F\text{-}bulk}$ ~ 0.066 – 0.097 Å^{-1}

$k_{F\text{-}bulk} < k_{F\text{-}2DEG} < k_{F\text{-}TSS}$ and $n_{2DEG} < 2\, n_{TSS}$

By estimating I_{TSS}:I_{2DEG}:I_{bulk}, **$\theta_{||}$ from only TSS** at low temperature is **~ 2.1 ± 0.39** (with bulk contribution) **~ 1.62 ± 0.18** (without bulk contribution)

If we assume TSS thickness ~ 1 nm, the 2D spin orbit torque efficiency
λ_{SOT} ~ 0.8-1.05 nm.
λ_{IREE} ~ 0.2-0.33 nm in Ag/Bi interface [Nat. Commun. **4**, 2944 (2013)]

NUS National University of Singapore

Wang *et al.*, PRL **114**, 257202 (2015)

178

Exotic spin Hall angles from topological insulators

spin Hall angle (θ_{SH}) = 2~3.5
ST-FMR (Cornell)

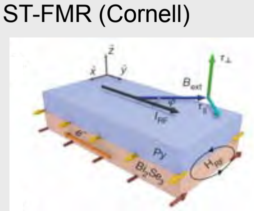

Nature **511**, 449 (2014)

θ_{SH} = 2 (low temp)
ST-FMR (NUS)

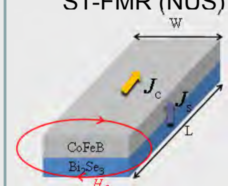

PRL **114**, 257202 (2015)

θ_{SH} = 140-425 (low temp)
spin-orbit switching (UCLA)

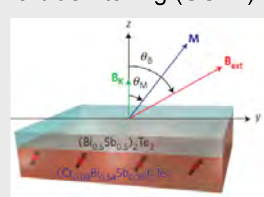

Nat. Mater. **13**, 699 (2014)

θ_{SH} = 0.01
Spin-pumping (Tohoku)

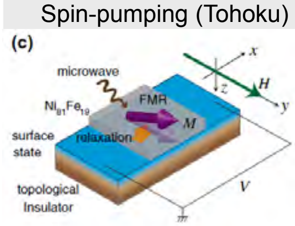

PRL **113**, 196601 (2014)

θ_{SH} = 0.01
Spin-pumping (NUS)

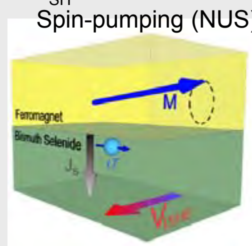

PRB **90**, 094403 (2014)

θ_{SH} = 0.01-0.4
Spin-pumping (Minnesota)

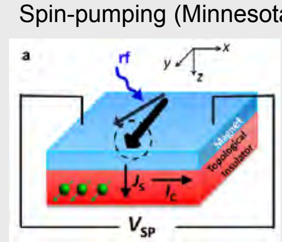

Nano Lett **15**, 7126 (2015)

180

Coexistence of surface states and Rashba bands

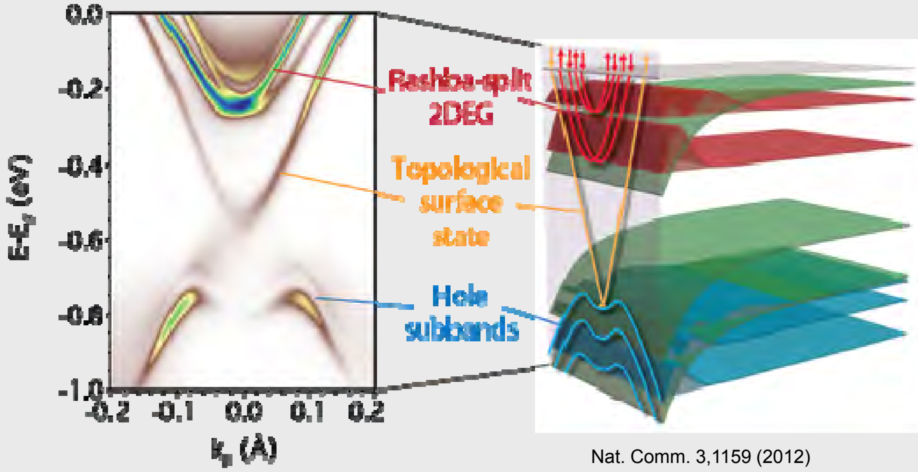

Nat. Comm. 3,1159 (2012)

Surface vs. bulk contribution to spin Hall angle ?

NUS National University of Singapore

Spin dependent photocurrents in Bi_2Se_3

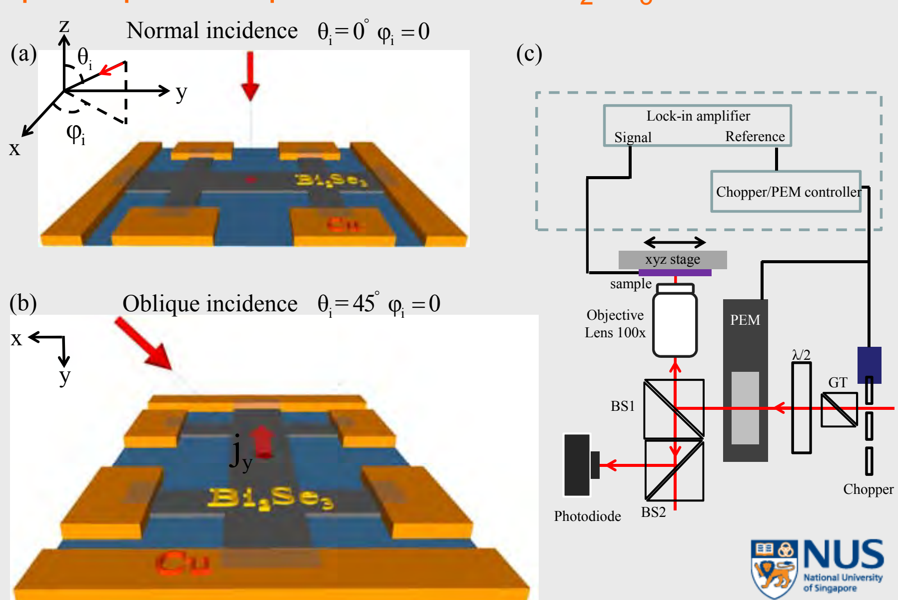

NUS National University of Singapore

Besbas et al., Adv. Opt. Mat. (in-press 2016)

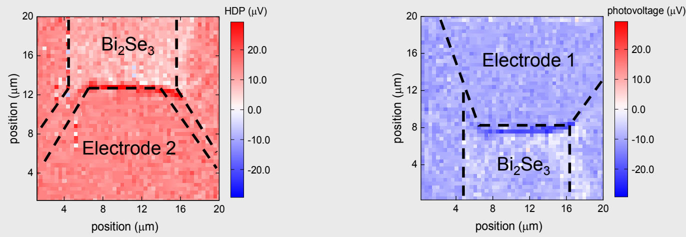

Experiment condition:
Circularly polarized light normal incidence on TI. Bias current is zero.

Observation:
The photocurrent generation at TI-metal interface.

Analysis:
1. The observed signal at the interface is due to electrostatic potential and hexagonal warping effect.
2. The smaller observed signal on TI is due to defected induced electrostatic potential.

Besbas et al., Adv. Opt. Mat. (in-press 2016)

199

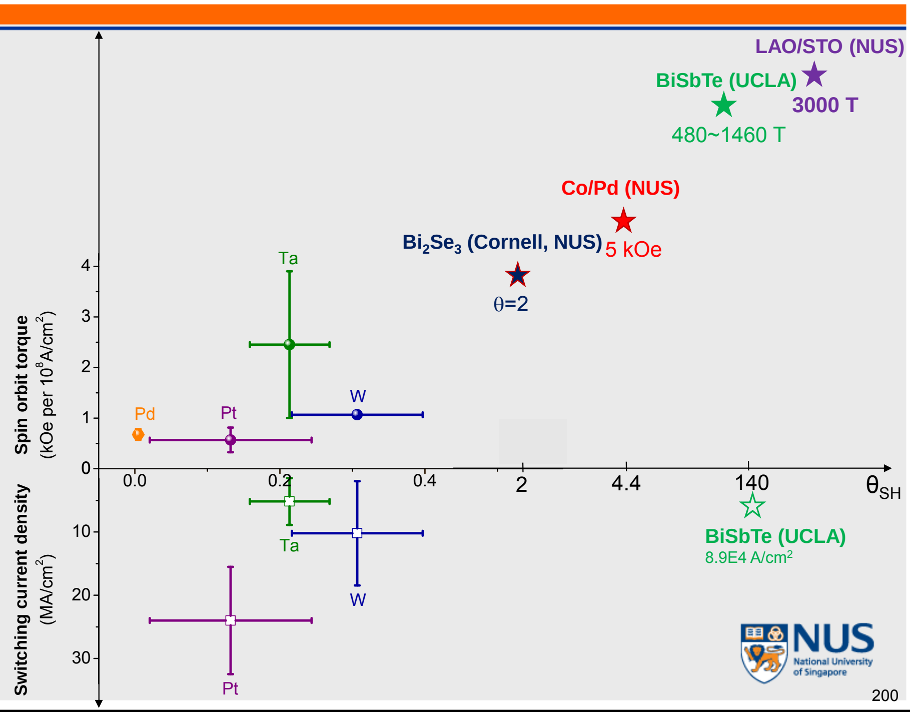

200

Open questions

- What is beyond band structures in Dirac/Weyl field?
- Can we make useful devices?
- Then what properties do we need to utilize?
  - Spintronics – spin momentum locking
  - Optoelectronics (THz) – intraband transition

NUS National University of Singapore

237

Dr. Yi Wang

Dr. Jean Besbas

Dr. Xuepeng Qiu

Dr. K. Narayanapillai

Dr. Yang Wu

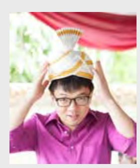

Dr. Qisheng Wang

Antonio Castro Neto (NUS)
Andre Geim (Manchster)
T. Venkatesan (NUS)
Seah Oh (Rutgers)
Aurelien Manchon (KAUST)
Lan Wang (RMIT Univ.)
K-J. Lee (Korea Univ.)

NUS National University of Singapore

238